https://doi.org/10.5194/angeo-2019-128
Preprint. Discussion started: 9 September 2019

Annales Geophysicae
Discussions
Open Access
EGU

A case study of the day-to-day occurrence of plasma irregularities in low-latitude ionosphere from multi-satellite observations

Weihua Luo[1], Chao Xiong[2], Zhengping Zhu[1], Shanshan Chang[1], and Xiao Yu[3]

[1] College of Electronic and Information Engineer, South-Central University for Nationalities, 430074 Wuhan, China.

[2] Helmholtz Centre Potsdam, GFZ German Research Centre for Geosciences, Telegrafenberg, 14473 Potsdam, Germany.

[3] China Research Institute of Radiowave Propagation, Qingdao, China

Correspondence: Weihua Luo (whlu@whu.edu.cn)

Abstract

Day-to-day variability of the occurrence of plasma irregularities in low-latitude ionosphere is still an open issue. In this study, we report the occurrence of post-sunset plasma bubbles and blobs detected by the First satellite of the Republic of China (ROCSAT-1) in the same longitude sector (170°E) on two successive days, under geomagnetically quiet and disturbed conditions, respectively. Multi-Low Earth orbit (LEO) missions, like the Defense Meteorological Satellite Program (DMSP) F13 and F15, the Gravity Recovery and Climate Experiment (GRACE) and the Challenging Mini-satellite Payload (CHAMP) satellites are used to study the preferable conditions for the occurrence of plasma bubbles and blobs. The observations from the CHAMP and GRACE show that the Equatorial Ionization Anomaly (EIA) was enhanced significantly before the occurrence of plasma irregularities on both two successive days. We suggest that the enhancement of post-sunset eastward electric field is the most important factor for the day-to-day development of the plasma irregularity in equatorial and low-latitude ionosphere. In addition, the meridional neutral wind plays an important role in the occurrence of low-latitude plasma blobs.

Keywords: low-latitude ionosphere; day-to-day variability; plasma bubble; plasma blob;

Key points:

https://doi.org/10.5194/angeo-2019-128
Preprint. Discussion started: 9 September 2019

Annales Geophysicae Discussions

- Low-latitude plasma bubbles and plasma blobs were detected by ROCSAT-1 on two successive days in 170°E region under quiet and disturbed conditions, respectively
- Equatorial Ionization Anomalies were enhanced significantly before the occurrence of the plasma irregularities on the two successive days
- Enhancement of the post-sunset eastward electric field plays an important role in the day-to-day occurrence of low-latitude plasma bubbles and plasma blobs

1. Introduction

The occurrence of plasma irregularities, including plasma density depletion (plasma bubble)/equatorial spread F (ESF) and plasma density enhancement (plasma blob), is one of particular phenomena after sunset in equatorial and low-latitude ionosphere, which display remarkable variations with local time, day-to-day, season, longitude, solar cycle, geomagnetic conditions and so on (Kelley, 2009). In general, the development of plasma bubble is thought to be initiated by the Rayleigh-Taylor (R-T) instability at the bottomside of F-region in equatorial ionosphere, the bubbles move upward and penetrates into topside ionosphere under the effect of $\mathbf{E}\times\mathbf{B}$. Based on multiple observations and numerical simulations, many reports have denoted that the pre-reversal enhancement (PRE) of the zonal electric field or vertical drift, neutral wind, solar flux, gravity wave (GW), Large Scale Wave Structure (LSWS) may affect the initiation of the plasma bubbles (e.g. Kelley, 2009; Tsunoda, 2010; Tsunoda et al., 2018). Up to date, the factors leading to the day-to-day occurrence of plasma bubbles are still an enigma.

The PRE vertical drift/zonal electric field is thought as a basic requirement for the development of post-sunset plasma bubble. Many studies have demonstrated that there is a “threshold” of vertical drift for the initiation of R-T instability (Huang, 2018, and references therein). However, the bubble may occur on the days when the drifts are lower than the “threshold”, or be absent on the days when the drifts beyond the “threshold” (e.g. Fejer et al., 1999; Lee et al., 2005).

Some studies also indicated that gravity waves, seeding R-T instability, may affect the day-to-day variability of plasma irregularity (e.g. Tsunoda, 2005; Aswathy and Manju, 2017; Tsunoda et al., 2018). Tsunoda et al. (2018) suggested that the controlling driver for bubble development may be related with the coupling between

https://doi.org/10.5194/angeo-2019-128
Preprint. Discussion started: 9 September 2019

the lower atmosphere and ionosphere, not vertical drift, such as the gravity waves (GW) or LSWS, planetary waves (PW), which are considered to last for several hours, from late afternoon to dusk and not easy to detect using ground-based observations (Tsunoda, 2005). The numerical simulations have shown that the forcing from lower atmosphere (e.g. GW) can initiate the R-T instability as a seed (Huang and Kelley, 1996; Krall et al., 2013), whether the growth of R-T instability can be amplified at later local time is not clear.

Thermospheric neutral wind is another candidate for the day-to-day variability of the plasma bubbles. Many experiments and numerical simulations have confirmed that the meridional and vertical neutral wind play an important role in the evolution of R-T instability and bubbles, depending on the directions of wind (Maruyama, 1988; Mendillo et al., 2001; Krall et al., 2009b; Sekar et al., 1994).There is no convincing evidences that meridional winds at dusk exert a strong influence on day-to-day post-sunset ESF onset (Mendillo et al., 2001).

Moreover, since the plasma blob was firstly reported by Watanabe and Oya (1986), the mechanism for the generation of plasma blob has not been well understood until now. Some studies indicated that the occurrence of plasma blob may be related with the plasma bubbles, occurred earlier at lower latitudes, due to the polarization electric field (Le et al., 2003; Huang et al., 2014; Yokoyama et al., 2007) and/or neutral wind (Krall et al., 2009a; Martinis et al., 2009; Park et al., 2003; Luo et al., 2018). Some studies showed that the plasma blob may generate independent on the occurrence of plasma bubble (Choi et al., 2012; Kil et al., 2011), and they contribute the formation of plasma blob to the traveling ionospheric disturbances (Kil et al., 2015; Martinis et al., 2009). Other studies proposed that the development of plasma blob may result from multi-mechanisms, because the blob can occur under the presence or the absence of the plasma bubble (Klenzing et al., 2011; Haaser et al., 2012).

However, previous studies on the possible factors for the day-to-day variability of plasma irregularities were statistical or from observations on a day or separate days. Thus, on the basis of multiple observations, more case studies in some successive days under similar and/or different geophysical conditions should be carried out to understand the day-to-day characteristics of plasma bubbles and blobs, and to investigate the possible factors or mechanisms for the day-to-day occurrence of

https://doi.org/10.5194/angeo-2019-128
Preprint. Discussion started: 9 September 2019

plasma bubbles and blobs. In this paper, we report the occurrences of plasma bubbles and plasma blobs detected by the First satellite of the Republic of China (ROCSAT-1) in 170°E longitude sector on two successive days, under quiet and disturbed conditions, respectively. Observations from Defense Meteorological Satellite Program (DMSP) F13 and F15 satellites, Challenging Mini-satellite Payload (CHAMP) and Gravity Recovery and Climate Experiment (GRACE) are also presented to discuss the possible factors on the day-to-day occurrence of plasma bubbles and plasma blobs.

2. Data descriptions

The DMSP is a series of satellites that fly in near-circular orbits (inclination: 98.7°) at about 840 km. The Special Sensor-Ions, Electrons, and Scintillation (SSIES) on board the satellites measures the ion and electron densities, temperatures and drifts. All DMSP satellites fly in Sun-synchronous orbits near either the 0600-1800 local time (LT) or the 0930-2130 LT meridians (Rich and Hairston, 1994). In this study, we use the data from the DMSP F13 and F15 satellites, whose orbit is on the 0600 LT and 0900 LT meridian, respectively.

The Ionospheric and Plasma Electrodynamics Instrument (IPEI) on board the ROCSAT-1, which was launched to a circular orbit on March 1999 with a 35° inclination orbital plane around 600 km, measures in-situ ion density, temperature and ion composition in the low-to-middle-latitude ionosphere (Yeh et al., 1999).

The CHAMP satellite was launched into an almost circular, near-polar orbit (inclination:87.3°) on 15 July, 2000, with an initial altitude of about 454 km. In 2003, the orbit decayed to about 400 km (Reigber et al., 2002). The Planar Langmuir Probe (PLP) on board the satellite measures the in-situ electron density and temperature per 15 seconds. The GRACE mission, including two spacecraft GRACE-A and GRACE-B, was launched into a polar-orbit (inclination:89°) on 17 March 2002, at an initial altitude of about 490 km (Tapley et al., 2004).

The electron density from PLP and the electron density derived from the K-band ranging (KBR) system between the GRACE two spacecraft (Xiong et al., 2010) have been validated by comparison with ground-based measurements at Jicamarca (McNamara et al., 2007) and European Incoherent Scatter radar (EISCAT), Millstone hill and Arecibo radars (Xiong et al., 2015), respectively. The electron densities from CHAMP and GRACE provide good opportunities to investigate the latitudinal

https://doi.org/10.5194/angeo-2019-128
Preprint. Discussion started: 9 September 2019

Annales Geophysicae Discussions

characteristics and variations of ionosphere at low- and middle latitudes, e.g., the Equatorial Ionization Anomaly (EIA) (e.g. Xiong et al., 2013).

3. Results

3.1 Observations from multi-satellites/ROCSAT-1

3.1.1 Plasma bubbles and plasma blobs detected by ROCSAT-1

Figure 1 presents the plasma bubbles in 170°E region recorded by ROCSAT-1 during 0940-0950 Universal Time (UT) on 17 August (left panel, I) and during 0949-0952 UT 18 August (right panel, II) 2003, respectively. Variations of three components of ion velocity, ion compostion, and ion temperature along the satellite trajectories are also displayed in the figure, and magnetic latitude, geographic longitude, UT, LT are noted at the bottom of figure. $V_{meridional}$ and V_{zonal} are the two components perpendicular to the field line in the meridional (upward) and zonal (eastward) direction, respectively. $V_{parallel}$ is field-aligned velocity.

As shown in Figure 1, in the same longitudinal region, plasma bubbles were recorded by ROCSAT-1 in two successive days, 17 and 18 August 2003.

On 17 August, in 180°E, the background density was about 2.75×10^5 cm^{-3}. At 7.46°N, the density decreased to about 9.4×10^4 cm^{-3}, and reached a minimum at 6.9°N (181°E), with the magnitude of 3.64×10^4 cm^{-3}. The density depletions were about 65.8% and 86.8%, respectively.

On 18 August, the density was about 1.71×10^5 cm^{-3} at 4.59°N, and 1.58×10^5 cm^{-3} at 4.14°N. The background density was about 6.12×10^5 cm^{-3}, which means the density depletions reached about 72.1% and 74.2%, respectively. At 1.69°N (180.08°E), the density reached a minimum of about 6.71×10^2cm^{-3}, the background density was about 3.5×10^5 cm^{-3}. The magnitude of density depletion exceeded 90%. At 1.52°N (180.37°E), the density was about 1.35×10^4 cm^{-3}, which means the depletion was about 96.1%.

On these two days, the bubbles moved poleward, westward and upward. However, there were differences between the bubbles on the two successive days. On 17 August, the O^+ composition inside the bubble showed increase or decrease, while O^+ composition inside the bubble on 18 August decreased.

https://doi.org/10.5194/angeo-2019-128
Preprint. Discussion started: 9 September 2019

Similar with Figure 1, Figure 2 presents the plasma blobs in 170°E region recorded by ROCSAT-1 during 1118-1129 UT on 17 August (left panel, I) and during 1128-1135 UT on 18 August (right panel, II) 2003, respectively.

As shown in Figure 2, in 170°E region, plasma blobs were recorded by ROCSAT-1 on two successive days, 17 and 18 August 2003, occurring after the earlier occurrences of the plasma bubbles.

On 17 August, in Region 1, at -6.58°N, the ion density increased to 2.35×10^5 cm^{-3}, the background density was about 1.0×10^5 cm^{-3}, which means the enhancement reached about 135%. In Region 2, the ion density was about 2.22×10^5 cm^{-3} at -3.81°N and 2.48×10^5 cm^{-3} at -3.5°N, which enhanced about 122% and 148% with respect to the background, respectively. In Region 3, the density was about 1.94×10^5 cm^{-3} at 0.86°N and 1.96×10^5 cm^{-3} at 0.98°N, respectively. The background density was about 1.38×10^5 cm^{-3}, the enhancements were about 40.6% and 42%, respectively.

In Region 4, the background density was about 1.86×10^5 cm^{-3} , the density decreased to about 1.41×10^5 cm^{-3} at 4.31°N, which means the depletion was 24.7%.

On 18 August, in Region 1, the ion density increased to 5.48×10^5 cm^{-3} at -16.27°N and 5.09×10^5 cm^{-3} at -15.96°N, the background density was about 4.38×10^5 cm^{-3}, which means the enhancement reached about 25.1% and 16.2%, respectively. In Region 2, the ion density was about 6.97×10^5 cm^{-3} at -14.15°N and 6.08×10^5 cm^{-3} at -14.62°N, which enhanced about 51.2% and 24.2% with respect to the background, with the magnitude of 4.61×10^5 cm^{-3}, respectively. In Region 3, the density was about 7.16×10^5 cm^{-3} at -12.1°N and 7.01×10^5 cm^{-3} at -12.02°N, respectively. The background density was about 4.68×10^5 cm^{-3}, the enhancements were about 53% and 49.8%, respectively.

In Region 4, there was small density disturbance, with the magnitude of about 10.2%. The drifts, composition and ion temperature show obvious fluctuations.

On 17 August, the O^+ composition inside the blob showed increase, while O^+ composition inside the bubble on 18 August decreased.

3.1.2 Tracks and observations of multi-satellites

To investigate the evolution of the plasma bubbles and blobs detected by ROCSAT-1, we also study the observations from other satellites in the same

https://doi.org/10.5194/angeo-2019-128
Preprint. Discussion started: 9 September 2019

Annales Geophysicae Discussions

longitudinal region. In Figure 3, we display the observations from ROCSAT-1, DMSP, GRACE and CHAMP satellites in 130-190°E region, and also the tracks of the satellites during 17-18 August 2003, at four different UT periods. The plasma bubbles and blobs recorded by satellites are also given in the figure, the red and green short lines represent the density enhancements (plasma blobs) and density depletions (plasma bubbles) encountered by the satellites, respectively.

From the Figure 3, we notice that the plasma bubbles were also detected in same region on 17 August by GRACE and DMSP at different altitudes, besides the ROCSAT-1, respectively. As displayed in Figure 3, the plasma bubbles were detected in 180°E regions on two successive days. On these two days, the bubbles moved westward, and after about 100 minutes, the plasma blobs were recorded in 170°E regions.

3.2 Observations from DMSP

Figure 4 shows the variations of ion density from DMSP F13 and F15 satellites along the satellite trajectories during 15-19 August 2003. The variations of longitude are also displayed in dashed lines.

It can be seen that the density around 0616 UT and 1026 UT at DMSP altitude increased significantly on 18 August 2003. On 17 August, it is interesting that the density showed obvious variations during different periods. The density around 0631 UT observed by DMSP F13 satellite was close to that around 0645 UT of 16 August. After more than 2 hours, around 0858 UT, the density in low-latitude region was larger obviously than that on other days.

3.3 EIA variations from CHAMP and GRACE

Figure 5 displays the variations of electron density along the satellite trajectories in low-latitude ionosphere from CHAMP and GRACE observations in 170°E sector during 1-22 August 2003, respectively. The satellite tracks are also shown in the figure. The local times measuring from CHAMP and GRACE were around 1900-2000 LT (after local sunset) and 2100-2130 LT, respectively.

In is seen that the densities on 17 and 18 August were larger above the crests and smaller at the trough with respect to that on other days of August 2003. On 17 and 18 August, EIA crests moved poleward, both at CHAMP altitude and GRACE altitude. Furthermore, similar with Luo et al. (2017), we calculate the EIA strength (Crest-to-

https://doi.org/10.5194/angeo-2019-128
Preprint. Discussion started: 9 September 2019

Annales Geophysicae Discussions

Trough Ratio, CTR) and asymmetry (ASY), which are calculated as *CTR=(N+S/2T)*, *ASY=(N-S)/((N+S)/2)*, respectively, shown in Figure 6. *N(S)* represents the density above the northern (southern) crest, *T* represents the density at the trough. When the EIA was not well developed, CTR is set as 1 and ASY is taken as 0, respectively.

The EIA stengths were enhanced significantly on 17 and 18 August, manifesting as the remarkable decrease of density at the trough and the increase of densities above the crests. CTR reached 50 on 17 August and 710 on 18 August, respectively. During the two days, especially on 18 August, EIA asymmetries at CHAMP altitude and GRACE altitude became more remarkable than that on 16 August, and 19 August.

3.4 Variations of [O/N2] ratio

Figure 7 displays the variations of Global Ultraviolet Imager (GUVI) [O/N_2] ratio during 16-19 August 2003.

Around the magnetic equator, the [O/N_2] ratio increased on 17 and 18 August, with respect to that on 16 August and 19 August.

4 Discussion

The occurrence of post-sunset plasma irregularities in equatorial and low-latitude ionosphere displays remarkable characteristics varying with day-to-day, season, solar cycle and so on. Generally, the plasma irregularity is preferable to occur during spring and fall equinox, under high solar flux (Aarons, 1993). Geomagnetic disturbance may promote or inhibit the occurrence of plasma irregularity (Martinis, 2005).

In linear theory of the development of R-T instability and plasma irregularity, background electric field and neutral wind are crucial factors for the initiation of R-T instability. In dipole coordinate system (*q*,*s*,*l*), the linear growth rate (γ) of R-T instability can be described as (e.g. Basu, 2002; Luo et al., 2013)

$$\gamma = \frac{1}{\eta_0 L_{nq}}\left(\frac{g}{\nu_{in}} + \frac{E_s}{B} - U_q + \frac{\nu_{in}}{\Omega_i}\frac{E_q}{B} + \frac{\nu_{in}}{\Omega_i}U_s\right) - \beta, \tag{1}$$

Where *Lnq* represents the scale length of vertical density gradient, ν_{in} is the ion-neutral collision frequency, Ω_i is the gyrofrequency of ions, E_s and E_q represent the background zonal and vertical electric field, *Uq* and *Us* represent the vertical and zonal wind, respectively.

https://doi.org/10.5194/angeo-2019-128
Preprint. Discussion started: 9 September 2019

Annales Geophysicae Discussions

As shown in Equation (1), the zonal electric field can strengthen or decrease the growth rate depending on the direction, which is thought as a basic requirement for the development of plasma irregularity after sunset. The growth rate can be affected directly by the vertical wind, which has been discussed by some studies (e.g. Sekar and Raghavarao, 1987; Raghavarao, 1999). Numerical simulations also have indicated that the nonlinear evolution of plasma bubbles would be amplified by vertical wind (Sekar et al., 1994; Krall et al., 2013; Yokoyama et al., 2019). It is well known that eastward electric field and downward wind would favor the development of R-T instability, which may play an important role in the day-to-day variability of the plasma irregularity.

In addition, the zonal electric field and meridional/vertical wind can affect the electrodynamics in equatorial and low-latitude ionosphere, such as the formation of EIA. Many studies have demonstrated that the variations of EIA, including EIA strength and asymmetry, are generally related with zonal electric field and meridional wind (Mendillo et al., 2001;Lin et al., 2005; Balan et al., 2018; Khadka et al., 2018). Thus, we can conclude the characteristics of zonal electric field and meridional wind in F-region from the EIA variations.

In this study, one interesting observation is that quite prominent plasma irregularities were detected during 17-18 August 2003, the relative low season of the occurrence of plasma bubbles, the density depletion or enhancement were not detected in same longitudinal sector on other days. Figure 8 presents an example for the variations of satellite tracks (top panel) and ion density (bottom panel) along the close ROCSAT-1 satellite trajectories on successive days.

The plasma irregularities were recorded on 17 and 18 August, and were absent on other days. The detailed density variations in 170°E region from ROCSAT-1 on 16 August and 19 August can be find in “Supplement”.

The other interesting result is that the plasma bubbles and blobs were detected on two successive days under different geophysical conditions, respectively. The geophysical conditions during the occurrences of the plasma irregularities are given in Figure 9. During 16-20 August, 2003, the variations of *Dst* index (a), K_p index (b), solar wind speed *Vsw* (c), the south-northern component of Interplanetary Magnetic Field (IMF) B_Z (d), and the Interplanetary Electric Field (IEF) E_y ($E_y = \boldsymbol{V}_{sw} \times \boldsymbol{B}$)(e), and also the variations of Prompt Penetration Electric Field (PPEF) and quiet plus

https://doi.org/10.5194/angeo-2019-128
Preprint. Discussion started: 9 September 2019

penetration electric field derived from the real-time model of the ionospheric electric fields (Manoji and Maus, 2012) at 170°E sector (f) are displayed, respectively. The red line represents the penetration electric field calculated from the IEF E_y and transfer function (Manoji and Maus, 2012), the green line represents the quiet background electric field plus the penetration electric field.

The storm sudden commencement (SSC) of the 17-20 August 2003 storm was at 1421 UT on 17 August. On 17 August, before the SSC, the *Dst* index did not show sudden variations and *Kp* indices were not more than 1. On 18 August, the *Dst* index dropped to a minimum (-148 nT) around 1600 UT, and K_p indices were no less than 6. After the SSC, E_y was westward and turned to east at about 1800 UT on 17 August. From Figure 8, it can be noted that the plasma irregularities detected by ROCSAT-1 occurred on a geomagnetically quiet day (17 August) and a disturbed day (18 August), during main phase of the storm, respectively.

On 17 August, as shown in Figure 8, before the SSC, the *Ey* was westward and the PPEFs were very small, which means that the background electric field may not be affected by the factors from the upper, such as PPEF.

On 18 August, the IEF E_y was always eastward and reached a maximum at 0800 UT, with a value of about 7.8 mV/m. The IEF would partially penetrate into the ionosphere as prompt penetration electric field (PPEF) with an efficiency of ~5 to 10% (Verkhoglyadova et al., 2008), with sudden variations of *Bz*. The IMF *Bz* was southward with sudden variations during 0000-0900 UT. It can be seen from Figure 8(f) that the penetration electric field was eastward during 0300-0800 UT, with the maximum of about 0.18 mV/m at 0530 UT. It means that the PPEF would affect the background electric field during 0300-0800 UT (local daytime), and the EIA may be enhanced due to PPEF.

As shown in Figures 5 and 6, on 17 and 18 August, the EIA derived from the CHAMP and GRACE observations showed remarkable enhancement. EIA strength is directly related with the zonal electric field. The enhanced eastward electric field, leading to a “super fountain” effect, would drive the EIA crests move toward the poles to higher latitudes, the density increase greatly above the crests while decreases near the magnetic equator (Lin et al., 2005; Lu et al., 2013; Balan et al., 2018). On the other hand, equatorward neutral wind may also strengthen the EIA (Lin et al., 2005; Balan et al., 2018), driving the crests move to the equator.

https://doi.org/10.5194/angeo-2019-128
Preprint. Discussion started: 9 September 2019

Annales Geophysicae Discussions Open Access EGU

From Figure 5, we can notice that EIA crests moved toward the poles on 17 and 18 August, with the remarkable increases of density above the crests and decrease near the magnetic equator. In addition, from Figure 4, the observations from DMSP F13 and F15 showed that the density on 17 August at DMSP altitude (840 km) was close to that on 16 August, and increased around 0858 UT with respect to that on 16 August, it means that the eastward electric field was strengthened during that period, which driven the density from the lower ionosphere to the higher altitude. Thus, it can be concluded that the density variations in EIA regions and motions of the crests indicated that the eastward electric field (PRE vertical drift) was enhanced after 0630 UT (around local sunset, before the occurrence of plasma bubbles) on 17 August in 170°E sector, leading to the EIA enhancement. As discussed before, the factor causing the increase of eastward electric field was not from the upper, which means that the EIA enhancement may be not associated with the storm.

Similar with the situation on 17 August, on 18 August, it can be concluded that the eastward electric field around local sunset was amplified before the occurrence of the plasma bubbles, which may be partially related with the PPEF.

Moreover, the EIA asymmetry on 17 and 18 August also showed obvious variations with respect to that on 16 August. On 17 August, EIA became more asymmetric with respect to that on 16 August, and the asymmetry on 18 August became more remarkable. The EIA asymmetry is generally related with the meridional neutral wind(Mendillo et al., 2001; Lin et al., 2005; Balan et al., 2018; Khadka et al., 2018), which modify the distribution of ionization with respect to the magnetic equator. Furthermore, it can be noted from Figure 5 that the characteristics of EIA asymmetry were different at different altitude. At CHAMP altitude, the ASY was positive, which means that the density above northern crest was larger that above the southern crest, and at GRACE altitude, the density above the nothern crest became smaller than that above the souther crest. The variations of the density above the crests at the different altitude means that the presence of the meridional wind on 17 and 18 August, with the altitudinal and/or horizontal gradient (Huba and Krall, 2013). Some reports have indicated that the trans-equatorial meridional wind may suppress the development of ESF/plasma bubbles (Maruyama, 1988; Mendillo et al., 2001; Krall et al., 2009b), and the plasma bubble is preferable to occur when the EIA is symmetric (Lee et al., 2005; Thampi et al., 2008). On 17 and 18 August, though the presence of the meridional wind, the plasma bubbles were recorded, which means that

https://doi.org/10.5194/angeo-2019-128
Preprint. Discussion started: 9 September 2019

the enhancement of eastward electric field is dominant for the occurrence of the plasma bubbles, whilethe meridional wind is not the dominant factor.

In addition, we notice that the plasma blobs were recorded on these two suceesive days. On these two days, as shown in Figure 1 and Figure 2, the plasma blobs were detected about 100 minutes after the occurrences of plasma bubble, and the variations of ion composition inside the blobs were similar with that inside the bubbles, which means that the blobs may be associated with the bubbles. Considering the relationship between the plasma bubble and blob, Huang et al. (2014) proposed that the polarization electric field due to the occurrence of plasma bubble would lead to the formation of plasma blob. Observational and numerical results also indicated that the meridional wind may cause the formation of plasma blob (Krall et al., 2009, 2010; Luo et al., 2018). In this study, it can be speculated that the presence of meridional wind on 17 and 18 August, from the variations of EIA shown in Figure 5. As Luo et al. (2018) proposed, under the effects of meridional wind, flowing from summer to winter hemisphere, in addition to the polarization electric field after the occurrence of plasma bubbles (Huang et al., 2014), the plasma blob could occur in winter hemisphere due to the accumulation of plasma in the low-latitude region.

There is another interesting result should be noted, as shown in Figure 7, the GUVI [O/N_2] ratio displayed the increase during 17-18 August in 150-180°E region. The compositional variability is mainly driven by both vertical and horizontal winds. The increase of [O/N_2] may be related with the downward wind (Rishbeth, 1998; Lin et al., 2005). Though the source of vertical wind in equatorial region is still not well understood (Larsen and Meriwether, 2012), the existences of vertical wind have been reported at different longitude sector (Biondi and Sipler, 1985; Raghavarao et al., 1993; Herrero and Meriwether, 1994). Raghavarao et al. (1993) proposed a possible source of vertical wind in equatorial region. When EIA enhanced, the pressure in EIA regions would be strengthened, and the enhanced pressure ridges would give rise to a downward wind in equatorial region and upward winds in crest regions (Raghavarao et al., 1993).

From Figures 4 and 5, we notice that EIAs were strengthened significantly with respect to other days in August. The vertical wind may be produced by the enhanced pressure in equatorial region, and the downward vertical wind would amplify the development of the R-T instability, and cause the increase of [O/N_2] ratio.

https://doi.org/10.5194/angeo-2019-128
Preprint. Discussion started: 9 September 2019

Annales Geophysicae Discussions

Thus, it can be concluded that the factors leading to the occurrence of plasma bubbles and blobs on 17 and 18 August are attributed to the enhanced eastward electric field after sunset, the vertical neutral wind due to the strengthen of EIA and the meridional neutral wind.

As mentioned before, the enhancement of eastward electric field on 17 August may be not from the upper, the enhancement of eastward electric field on 18 August may be partially from the PPEF. Other sources for the enhancement are from the below, such as the LSWS, PW and GW. The wave structure, manifesting itself as the height oscillations of the bottomside F layer at daytime, becomes amplified towards post-sunset hours. The vertical and zonal winds, associated with gravity wave propagating zonally and slant upward, would generate a polarization electric field. A vertical perturbation wind (ΔU_Z) produces the zonal polarization electric field (ΔEy) as ΔEy=-$\Delta U_Z \times B_0$. Some observations have demonstrated that the propagating LSWS may generate polarization electric fields and enhance the PRE vertical drift (Fagundes et al., 1999; Abdu et al., 2015; Ajith et al., 2018; Abdu, 2019), and many studies have showed the occurrence of plasma irregularities may be related with the LSWS (e.g. Thampi et al., 2009; Tsunoda et al., 2018).

It can be speculated that the enhancement of eastward electric field on 17 August may be associated the presence of propagating LSWS or GW. Unfortunately, we cannot find any evidences to study the presence of LSWS in the ionosphere. The relationship between the LSWS and the enhancement post-sunset electric field/vertical drift, and also the occurrence of plasma bubbles need to be further studied from multiple observations.

In conclusion, the occurrences of the plasma bubbles and blobs in this case on both two successive days can be concluded as: 1) at first, the PRE vertical drift (eastward electric field) was enhanced due to the factors from below on 17 August, e.g. gravity waves, and the PPEF on 18 August, respectively; 2) EIA became stronger and R-T instability was initiated under the effect of the enhanced post-sunset eastward electric field, in addition to the downward neutral wind resulting from the strengthened EIA, leading to the occurrence of the plasma bubbles; 3) under the effect of the meridional neutral wind, EIA became more asymmetric, and the plasma blobs occurred on 17 and 18 August. In a word, the enhancement of post-sunset eastward electric field is the most important for the occurrence of plasma bubble

https://doi.org/10.5194/angeo-2019-128
Preprint. Discussion started: 9 September 2019

Annales Geophysicae
Discussions
Open Access

under quiet conditions, giving rise to the vertical wind, whatever resulting from the below or above, such as LSWS or PPEF, even in the low season of the occurrence of plasma irregularity. The meridional wind may be not the dominant factor for the occurrence of the plasma bubble, but for the plasma blob.

5 Conclusions

In this paper, we present the occurrence of plasma bubbles and blobs in the same longitude sector (170°-180°E) on the two successive days, not the high season of the occurrence of plasma irregularity, under quiet and disturbed conditions, respectively. Observations from multi-satellites are used to study the possible factors accounting for the occurrence of plasma irregularity. The main remarks can be summarized as below,

1) On a quiet day, 17 August 2003, after local sunset, the plasma bubbles in 180°E sector were detected by GRACE, ROCSAT-1 and DMSP F15 satellites. After about 100 minutes, the plasma blobs in 170°E sector were detected by ROCSAT-1 in low-latitude region due to the westward motion of plasma irregularities.

On 18 August 2003, during the main phase of the storm, the plasma bubbles in 180°E sector were firstly recorded, and the plasma blobs in 170°E sector were also detected after about 100 minutes by ROCSAT-1.

2) Observations from CHAMP and GRACE indicated that EIAs were enhanced significantly before the occurrence of plasma bubbles on the two successive days with respect to that on other days. EIA asymmetry also displayed remarkable variations.

3) [O/N_2] ratio also showed the increase on 17 and 18 August 2003. The increase can be attributed to the downward wind, generating from the enhancement of EIA strength.

4) The remarkable enhancement of EIA strength under quiet condition can be attributed to the enhancement post-sunset eastward electric field, due to the factors from below, such as the gravity waves at the lower atmosphere, which need to be further studied. In result, the enhanced EIA give rise to a downward wind in equatorial region, which favor the initiation of R-T instability and occurrence of plasma bubble. The downward wind also lead to the enhancement of [O/N_2] ratio.

The enhancement of post-sunset eastward electric field is suggested to be the most important for the day-to-day development of plasma irregularity, which could lead to the rapid rise of F-layer, EIA enhancement, and also the generation of vertical wind in equatorial region.

5) Meridional wind plays an important role in the occurrence of the plasma blob in low-latitude ionosphere. Under the effects of the meridional neutral wind, in addition to the polarization electric field from the occurrence of plasma bubbles, the plasma blobs occurred on two successive days.

Acknowledgements. The work is supported by National Natural Science Foundation of China (41474134, 41474135, 41704161). We acknowledge UCAR, NCU, UT at Dallas, ACE science centre, JHU for providing the satellites data and GUVI [O/N_2] data, respectively.

Data availability. The *Dst* and K_p data are downloaded from World Data Center at Kyoto (http://swdcdb.kugi.kyoto-u.ac.jp/dstdir/index.html). The ROCSAT-1 data can be downloaded from NCU (http://sdbweb.ss.ncu.edu.tw/ipei_download.html). The DMSP data can be downloaded from the Center for Space Science at the University of Texas at Dallas (http://cindispace.utdallas.edu/DMSP/dmsp_data_at_utdallas.html). The CHAMP and GRACE data can be downloaded from CDAAC (http://cdaac-www.cosmic.ucar.edu/cdaac/products.html). The Interplanetary Magnetic Field and Solar wind speed are downloaded from the ACE center (http://www.srl.caltech.edu/ACE/ASC/). The GUVI [O/N_2] ratio are download from http://guvitimed.jhuapl.edu/data_on2_info. The real-time model of the ionospheric electric field can be accessed from CIRES (http://geomag.org/models/PPEFM/RealtimeEF.html).

Author contribution. WL analyzed the data and prepared the manuscript, CX discussed the results and modified the manuscript, ZZ, SC and XY help to analyze the data and discussed the results. All the authors read and approved the final manuscript.

Competing interests. The authors declare that they have no conflict of interest.

References

Aarons, J.: The longitudinal morphology of equatorial F layer irregularities relevant to their occurrence, Space Sci. Rev., 63, 209, https://link.springer.com/article/10.1007/BF00750769, 1993.

https://doi.org/10.5194/angeo-2019-128
Preprint. Discussion started: 9 September 2019

Annales Geophysicae Discussions
Open Access
EGU

Abdu, M.A.: Day-to-day and short-term variabilities in the equatorial plasma bubble/spread F irregularity seeding and development, Prog. in Earth and Plan. Sci., 6(11), https://doi.org/10.1186/s40645-019-0258-1, 2019.

Abdu, M.A., de Souza J.R., Kherani E.A., Batista I.S., MacDougall J.W., Sobral J.H.A.: Wave structure and polarization electric field development in the bottomside F layer leading to postsunset equatorial spread F, J. Geophys. Res., 120, 6930-6940, https://doi.org/10.1002/2015JA021235, 2015.

Ajith, K.K., Ram S.T., Carter B.A., Kumar S. S., Yamamoto M., Yokoyama T., Gurubaran S., Sripathi S., Hozumi K., Groves K., Caton R.G.: Unseasonal development of post-sunset F-region irregularities over Southeast Asia on 28 July 2014: 2. Forcing from below?, Prog. in Earth and Plan. Sci., 5(60), https://doi.org/10.1186/s40645-018-0218-1, 2018.

Aswathy, R.P., and Manju G.: Gravity wave control on ESF day-to-day variability: An empirical approach, J. Geophys. Res., 122, 6791-6798, https://doi.org/10.1002/2017JA023983, 2017.

Basu, B.: On the linear theory of equatorial plasma instability: Comparison of different descriptions, J. Geophys. Res., 107, A8, 1199, https://doi.org/10.1029/2001JA000317, 2002.

Biondi, M.A. and Sipler D.P.: Horizontal and vertical winds and temperatures in the equatorial thermosphere: Measurements from Natal, Brazil during August-September 1982, Plan. and Space Sci., 33, 817-823, https://doi.org/10.1016/0032-0633(85)90035-2, 1985.

Choi, H.S., Kil H., Kwak Y.S., Park Y.D., and Cho K.S.: Comparison of the bubble and blob distribution during the solar minimum, J. Geophys. Res., 117, A04314, https://doi.org/10.1029/2011JA017292, 2012.

Fagundes, P.R., Sahai Y., Batista I.S., Abdu M.A., Bittencourt J.A., Takahashi H.: Observations of day-to-day variability in precursor signatures to equatorial F-region plasma depletions, Ann. Geophys., 17, 1053-1063, https://doi.org/10.1007/s00585-999-1053-x, 1999.

Fejer, B.G., Scherliess L., and de Paula E.R.: Effects of the vertical drift velocity on the generation and evolution of equatorial spread F, J. Geophys. Res., 104, A9, 19859-19869, https://doi.org/10.1029/1999JA900271, 1999.

https://doi.org/10.5194/angeo-2019-128
Preprint. Discussion started: 9 September 2019

Herrero, F.A., and Meriwether J.W.: The 630 nm MIG and the vertical neutral wind in the low latitude nighttime thermosphere, Geophys. Res. Lett., 21(2), 97-100, h ttps://doi.org/10.1029/93GL03115, 1994.

Haaser, R.A., Earle G.D., Heelis R.A., Klenzing J., Stoneback R., Coley W.R., and Burrell A.G.: Characteristics of low-latitude ionospheric depletions and enhancements during solar minimum, J. Geophys. Res., 117, A10305, https://doi.org/10.1029/2012JA017814, 2012.

Huang, C.S., and Kelley M.C.: Nonlinear evolution of equatorial spread F 2. Gravity wave seeding of Rayleigh-Taylor instability, J. Geophys. Res., 101, A1, 293-302, https://doi.org/10.1029/95JA02210, 1996.

Huang, C.S., Le G., de La Beaujardiere, Roddy P.A., Hunton D.E., Pfaff R.F., and Hairston M.R.: Relationship between plasma bubbles and density enhancements: Observations and interpretation, J. Geophys. Res., 119, 1325-1336, https://doi.org/10.1002/2013JA019579, 2014.

Huang, Chaosong: Effects of the postsunset vertical plasma drift on the generation of equatorial spread F, Prog. in Earth and Plan. Sci., 5(3), https://doi.org/ 10.1186/s40645-017-0155-4, 2018.

Huba, J.D., and Krall J.: Impact of meridional winds on equatorial spread F: Revisited, Geophys. Res. Lett., 40, 1268-1272, https://doi.org/10.1002/grl.50292, 2013.

Kelly, M.C.: The Earth's Ionosphere: Plasma Physics & Electrodynamics. International geophysics series, second ed. San Diego, California, ISBN:978-0-12-088425-4, Academic, 2009.

Khadka, S.M., Valladares C.E., Sheehan R., Gerrard A.J.: Effects of electric field and neutral wind on the asymmetry of Equatorial Ionization Anomaly, Radio Sci., 53, 683-697, https://doi/10.1029/2017RS006428, 2018.

Kil, H., Kwak Y.S., Lee W.K., Miller E.S., Oh S.J., and Choi H.S.: The causal relationship between plasma bubbles and blobs in the low-latitude F region during a solar minimum, J. Geophys. Res., 120, 3961-3969, https://doi.org/10.1002/2014JA020847, 2015.

Kil, H., Choi H.S., Heelis R.A., Paxton L.J., Coley W.R., and Miller E.S.: Onset condition of bubbles and blobs: A case study on 2 March 2009, Geophys. Res. Lett., 38, L06101, https://doi.org/10.1029/2011GL046885, 2011

https://doi.org/10.5194/angeo-2019-128
Preprint. Discussion started: 9 September 2019

Annales Geophysicae
Discussions

Klenzing, J.H., Rowland D.E., Pfaff R.F., Le G., Freudenreich H., Haaser R.A., Burrell A.G., Stoneback R.A., Coley W.R., and Heelis R.A.: Observations of low-latitude plasma density enhancements and their associated with plasma drifts, J. Geophys. Res., 116, A09324, https://doi.org/10.1029/2011JA016711, 2011.

Krall, J., Huba J.D., and Martinis C.R.: Three-dimensional modeling of equatorial spread F airglow enhancements, Geophys. Res. Lett., 36, L10103, https://doi.org/10.1029/2009GL038441, 2009a.

Krall, J., Huba J. D., Joyce G., and Zalesak S. T.: Three-dimensional simulation of equatorial spread-F with meridional wind effects, Ann. Geophys., 27, 1821–1830, https://doi.org/10.5194/angeo-27-1821-2009, 2009b.

Krall, J., Huba J.D., and Fritts D.C.: On the seeding of equatorial spread F by gravity waves, Geophys. Res. Lett., 40, 661-664, https://doi.org/10.1002/GRL.50144, 2013.

Larsen, M.F. and Meriwether J.W.: Vertical winds in the thermosphere, J. Geophys. Res., 117, A09319, https://doi.org/10.1029/2012JA017843, 2012.

Le, G., Huang C.S., Pfaff R.F., Su S.Y., Yeh H.C., Heelis R.A., Rich F.J., and Hairston M.: Plasma density enhancements associated with equatorial spread F: ROCSAT-1 and DMSP observations, J. Geophys. Res., 108, A8, https://doi.org/10.1029/2002JA009592, 2003.

Lee, C.C., Liu J.Y., Reinisch B.W., Chen W.S., and Chu F.D.: The effects of the pre-reversal drifts, the EIA asymmetry, and magnetic activity on the equatorial spread F during solar maximum, Ann. Geophys., 23, 745-751, https://doi.org/10.5194/angeo-23-745-2005, 2005.

Lin, C.H., Richmond A.D., Heelis R.A., Bailey G.J., Lu G., Liu J.Y., Yeh H.C., Su S.Y.: Theoretical study of the low- and midlatitude ionospheric electron density enhancement during the October 2003 superstorm: Relative importance of the neutral wind and the electric field, J. Geophys. Res., 110, A12312, https://doi.org/10.1029/2005JA011304, 2005.

Lu, G., Huba J.D., and Valladares C.: Modeling ionospheric super-fountain effect on the coupled TIMEGCM_SAMI3, J. Geophys. Res., 118, 2527-2535, https://doi.org/10.1002/jgra.50256, 2013.

Luo Weihua, Xu J.S., Zhu Z.P.: Theoretical modeling of the occurrence of equatorial and low-latitude ionospheric irregularity and scintillation, Chinese J. Geophys. (in Chinese), 56(9), 2892-2905, https://doi.org/10.6038/cjg20130903, 2013.

Luo Weihua, Zhu Zhengping, Xiong Chao, and Chang Shanshan: The response of equatorial ionization anomaly in 120°E to the geomagnetic storm of 18 August 2003 at different altitudes from multiple satellite observations, Space Weather, 15, 1588-1601. https://doi.org/10.1002/2017SW001710, 2017.

Luo Weihua, Xiong Chao, Zhu Zhengping, and Mei Xuefei: Onset condition of plasma density enhancements: A case study for the effects of meridional wind during 17-18 August 2003, J. Geophys. Res., 123, 6714-6726, https://doi.org/10.1029/2018JA025191, 2018.

Manoj, C., and Maus S.: A real-time forecast service for the ionospheric equatorial zonal electric field, Space Weather, 10, S09002, https://doi.org/10.1029/2012SW000825, 2012.

Maruyama, T.: A diagnostic model for equatorial spread-F 1. Model description and application to electric field and neutral wind effects, J. Geophys. Res. 93, 14611–14622, https://doi.org/10.1029/JA093iA12p14611, 1988

Martinis, C., Baumgardner J., Mendillo M., Su S.Y., and Aponte N.: Brightening of 630.0 nm equatorial spread-F airglow depletions, J. Geophys. Res., 114, A06318, https://doi.org/10.1029/2008JA013931, 2009.

Martinis, C.R., Mendillo M.J., Aarons J.: Toward a synthesis of equatorial spread F onset and suppression during geomagnetic storms, J. Geophys. Res., 110, A07306, https://doi.org/10.1029/2003JA010362, 2005.

McNamara, L., Cooke D.L., Valladares C.E., Reinisch B.W.: Comparison of CHAMP and Digisonde plasma frequencies at Jicamarca, Peru, Radio Sci., 42, RS2005, http://dx.doi.org/10.1029/2006RS003491, 2007.

Mendillo, M., Meriwether J., Biondi M.: Testing the thermospheric neutral wind suppression mechanism for day-to-day variability of equatorial spread F, J. Geophys. Res., 106(A3), 3655–3663, https://doi.org/10.1029/2000JA000148, 2001.

Park, J., Min K.W., Lee J.J., Kil H., Kim V.P., Kim H.J., Lee E., Lee D.Y.: Plasma blob events observed by KOMPSAT-1 and DMSP F15 in the low latitude nighttime upper ionosphere, Geophys. Res. Lett., 30(21), 2114, https://doi.org/10.1029/2003GL018249, 2003.

https://doi.org/10.5194/angeo-2019-128
Preprint. Discussion started: 9 September 2019

Annales Geophysicae Discussions

Verkhoglyadova, O.P., Tsurutani B.T., Mannucci A.J., Saito A., Araki T., Anderson D., Abdu M., Sobral J.H.A.: Simulation of PPEF effects in dayside low-latitude ionosphere for the October 30, 2003, superstorm, Geophysical Monograph 181, Midlatitude ionospheric dynamics and disturbances, 169-178, 2008.

Watanbe, S. and Oya H.: Occurrence characteristics of low latitude ionosphere irregularities observed by impendence probe on board the Hinotori satellite, J. Geomag. Geoelectr., 38, 125-149, https://doi.org/10.5636/jgg.38.125 , 1986.

Raghavarao, R., Hoegy W.R., Spencer N.W., and Wharton L.E.: Neutral temperature anomaly in the equatorial thermosphere-A source of vertical winds, Geophys. Res. Lett., 20(11), 1023-1026, https://doi.org/10.1029/93GL01253 , 1993.

Raghavarao, R., Suhasini R., Mayr H.G., Hoegy W.R., Wharton L.E.: Equatorial spread-F (ESF) and vertical winds, J. Atmos. and Sol-Terr. Phys., 61, 607-617, https://doi.org/10.1016/S1364-6826(99)00017-6, 1999.

Reigber, C., Lühr H., and Schwintzer P.: CHAMP mission status, Adv. in Space Res., 30, 129-134, https://doi.org/10.1016/S0273-1177(02)00276-4, 2002.

Sekar, R., Suhasini R., and Raghavarao R.: Effects of vertical winds and electric fields in the nonlinear evolution of equatorial spread F, J. Geophys. Res., 99(A2), 2205-2213, https://doi.org/10.1029/93JA01849, 1994.

Sekar, R., and Raghavarao R.: Role of vertical winds on the Rayleigh-Taylor mode instabilities of the night-time equatorial ionosphere, J. Atmos. and Terr. Phys., 49(10), 981-985, https://doi.org/10.1016/0021-9169(87)90104-8, 1987.

Tapley, B.D., Bettadpur S., Watkins M., and Reigber C.: The gravity recovery and climate experiment: Mission overview and early results, Geophys. Res. Lett., 31, L09607, https://doi.org/10.1029/2004GL019920, 2004.

Thampi, S.V., Ravindran S., Pant T.K., Devasia C.V., and Sridharan R.: Seasonal dependence of the “forecast parameter” based on the EIA characteristics for the prediction of Equatorial Spread F (ESF), Ann. Geophys., 26, 1751-1757, https://doi.org/10.5194/angeo-26-1751-2008, 2008.

Thampi, S.V., Yamamoto M., Tsunoda R.T., Otsuka Y., Tsugawa T., Uemoto J., Ishii M.: First observations of large-scale wave structure and equatorial spread F using CERTO radio beacon on the C/NOFS satellite, Geophys. Res. Lett., 36, L18111, https://doi.org/10.1029/2009GL039887, 2009.

https://doi.org/10.5194/angeo-2019-128
Preprint. Discussion started: 9 September 2019

Tulasi Ram, S., Yamamoto M., Tsunoda R.T., Chau H.D., Hoang T.L., Damtie B., Wassaie M., Yatini C.Y., Manik T., Tsugawa T.: Characteristics of large-scale wave structure observed from African and Southeast Asian longitudinal sectors, J. Geophys. Res., 119, 2288-2297, https://doi.org/10.1002/2013JA019712, 2014.

Tsunoda, R.T.: On the enigma of day-to-day variability in equatorial spread F, Geophys. Res. Lett. , 32, L08103, https://doi.org/10.1029/2005GL022512, 2005.

Tsunoda, R.T.: On seeding equatorial spread F during solstice, Geophys. Res. Lett., 37, L05102, https://doi.org/10.1029/2010GL042576,2010.

Tsunoda, R.T., Bubenik D.M., Thampi S.W., and Yamamoto M.: On large-scale wave structure and equatorial spread F without a post-sunset rise of the F layer, Geophys. Res. Lett., 37, L07105, https://doi.org/10.1029/2009GL042357, 2010.

Tsunoda, R.T., Saito S., Nguyen T.T.: Post-sunset rise of equatorial F layer-or upwelling growth?, Prog. in Earth and Plan. Sci., 5(22), https://doi.org/10.1186/s40645-018-0179-4, 2018.

Xiong, C., Park J., Lühr H., Stolle C., Ma S.Y.: Comparing plasma bubble occurrence rates at CHAMP and GRACE altitudes during high and low solar activity, Ann. Geophys., 28, 1647-1658, https://doi.org/10.5194/angeo-28-1647-2010, 2010.

Xiong, C., Lühr, H., and Ma S.Y.: The magnitude and inter-hemispheric asymmetry of equatorial ionization anomaly- based on CHAMP and GRACE observations, J. Atmos. and Sol-Terr. Phys., (105-106), 160-169, https://doi.org/10.1016/j.jastp.2013.09.010, 2013.

Xiong, C., Lühr H., and Fejer B. G.: Validation of GRACE electron densities by incoherent scatter radar data and estimation of plasma scale height in the topside ionosphere, Adv. in Space Res., 55, 8, 2048–2057, https://doi.org/10.1016/j.asr.2014.07.022, 2015.

Yeh, H.C., Su S.Y., Yeh Y.C., Wu J.M., Heelis R.A., and Holt B.J.: Scientific mission of the IPEI payload onboard ROCSAT-1, Terres., Atmos. and Ocean. Sci., 10(1-1), 19-42, https://doi.org/10.3319/TAO.1999.10.S.19(ROCSAT), 1999.

Yokoyama, T., Su S.Y., and Fukao S.: Plasma blobs and irregularities concurrently observed by ROCSAT-1 and equatorial atmosphere radar, J. Geophys. Res., 112, A05311, https://doi.org/10.1029/2006JA012044, 2007.

Yokoyama, T., Jin H., Shinagawa H., Liu H.: Seeding of equatorial plasma bubbles by vertical neutral wind, Geophys. Res. Lett., https://doi.org/10.1029/2019GL083629, 2019.

https://doi.org/10.5194/angeo-2019-128
Preprint. Discussion started: 9 September 2019

Annales Geophysicae
Discussions
Open Access
EGU

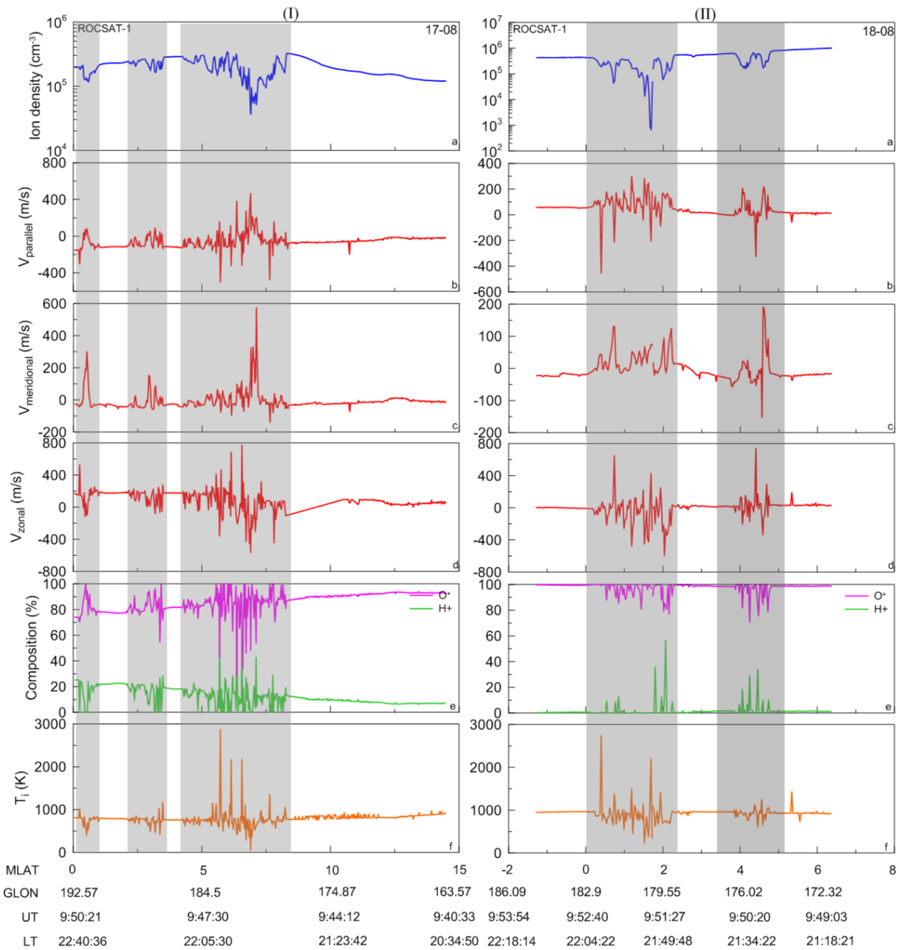

Figure 1. The ion density, drift, composition and temperature observed from ROCSAT-1 along the satellite trajectories in 170°E sector during 0940-0950 UT on 17 August 2003 (left panel, I) and during 0949-0952 UT on 18 August 2003 (right panel, II), respectively. $V_{parallel}$ is the field-aligned component, $V_{meridional}$ is meridional, V_{zonal} is zonal.

https://doi.org/10.5194/angeo-2019-128
Preprint. Discussion started: 9 September 2019

Annales Geophysicae Discussions
Open Access

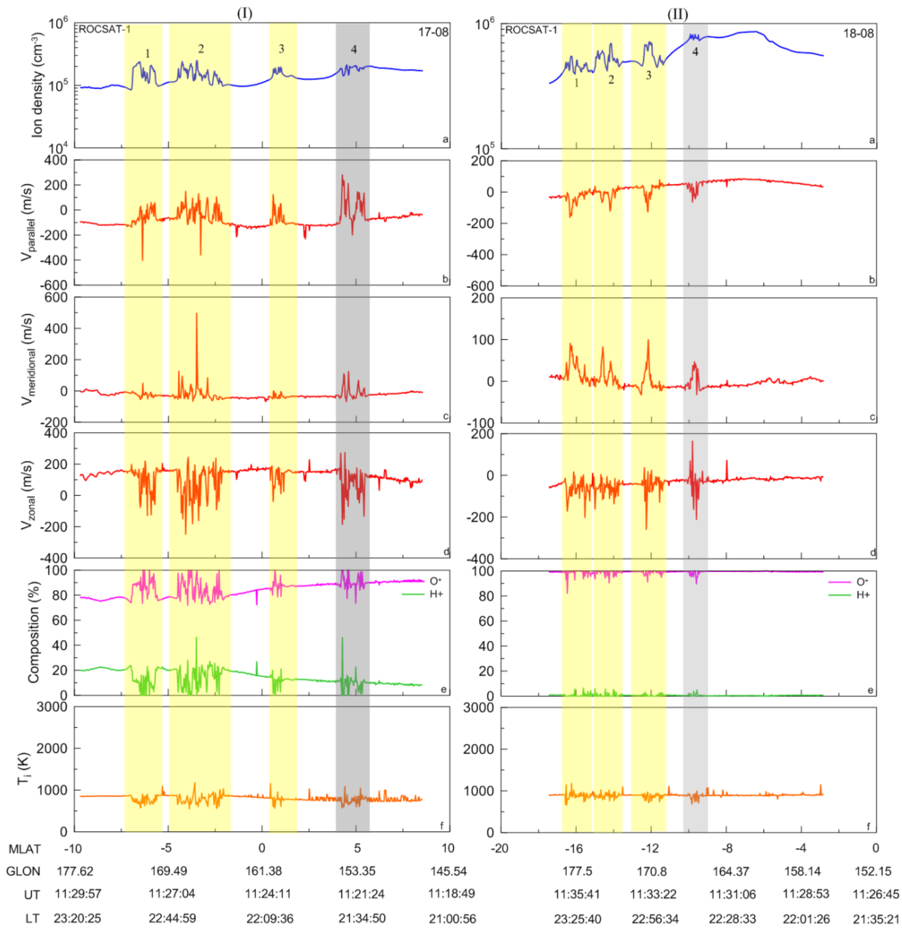

Figure 2. The ion density, drift, composition and temperature observed from ROCSAT-1 along the satellite trajectories in 170°E sector during 1118-1129 UT on 17 August 2003 (left panel, I) and during 1128-1135 UT on 18 August 2003 (right panel, II), respectively.

https://doi.org/10.5194/angeo-2019-128
Preprint. Discussion started: 9 September 2019

Annales Geophysicae
Discussions
Open Access

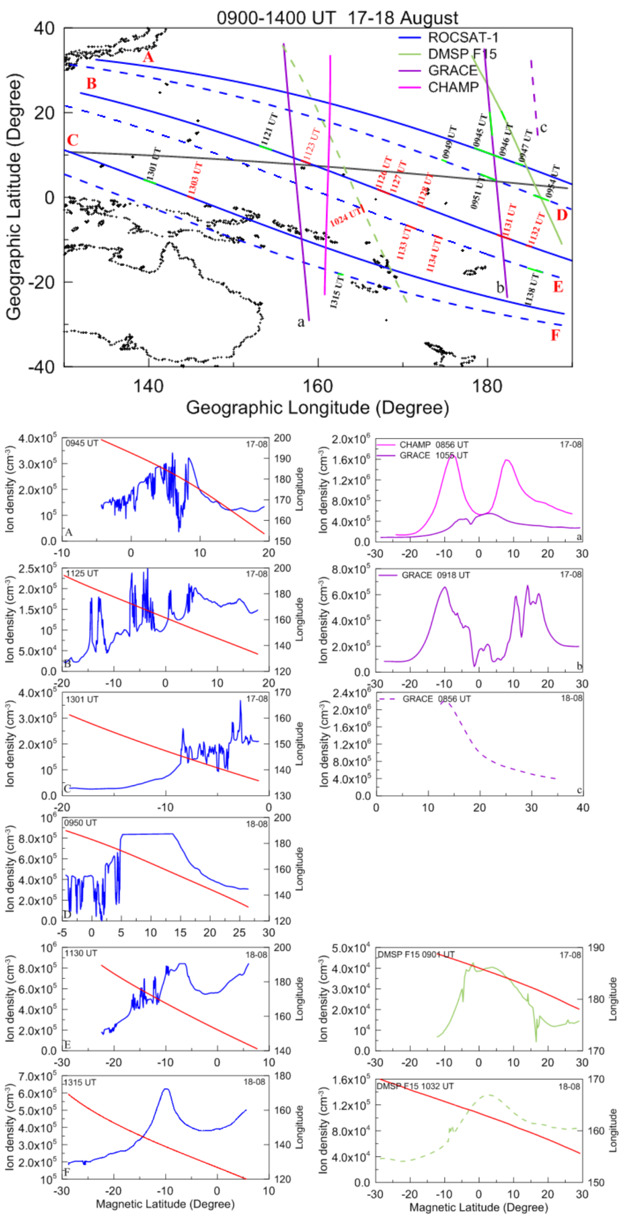

Figure 3. During 0900-1400 UT, on 17 and 18 August, the regional map at 130-190°E longitude sector including the trajectories of DMSP, ROCSAT-1, GRACE, CHAMP satellites (top panel), and the variations of ion density along the satellite trajectories (bottom panel). The red and green short lines represent the density enhancements and the density depletions recorded by the satellites, respectively. The solid lines represent the observations on 17 August, while the dashed lines represent the observations on 18 August.

https://doi.org/10.5194/angeo-2019-128
Preprint. Discussion started: 9 September 2019

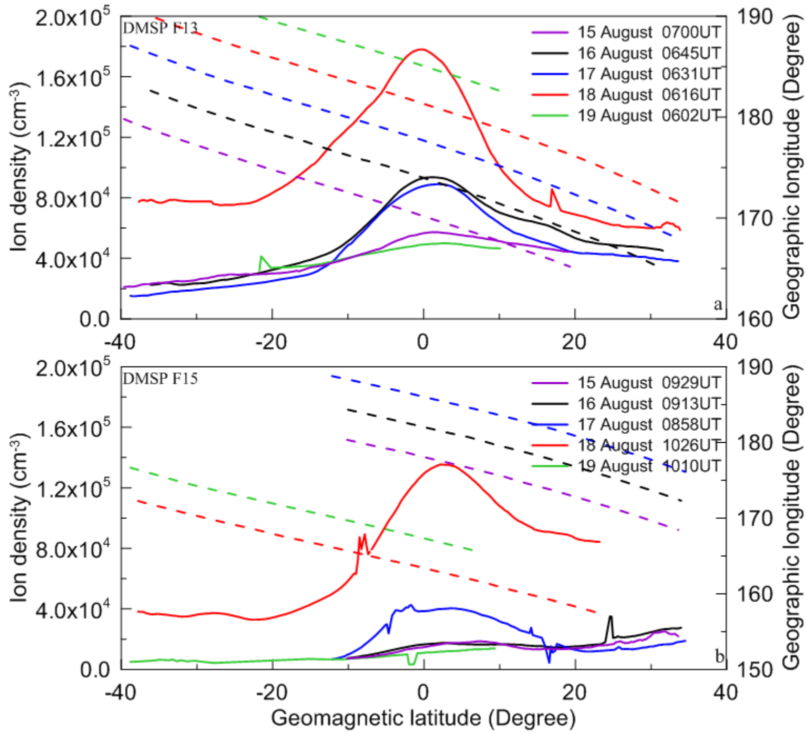

Figure 4. Variations of ion density and longitudinal tracks from DMSP F13 (a) and F15 (b) along the satellite trajectories during 15-19 August 2003. The solid lines represent the ion density, the dashed lines represent the longitudinal tracks.

https://doi.org/10.5194/angeo-2019-128
Preprint. Discussion started: 9 September 2019

Annales Geophysicae Discussions

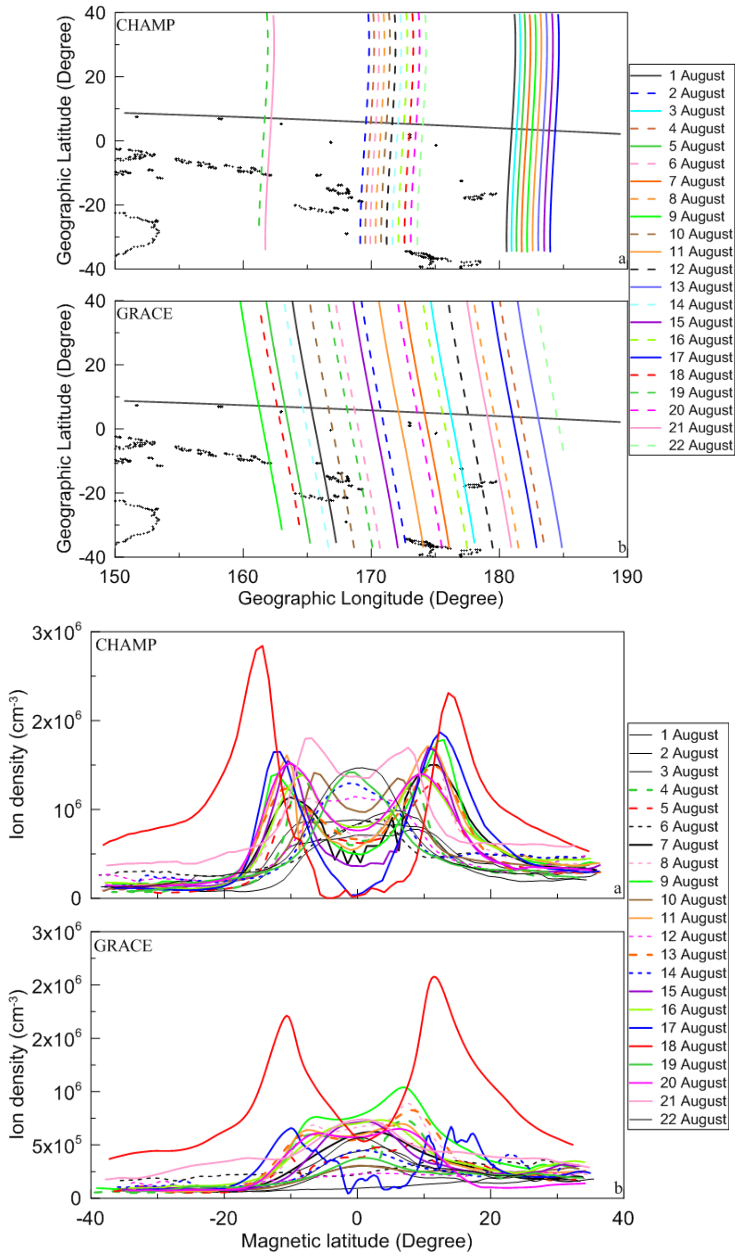

Figure 5. During 1-22 August 2003, in 170°E region, the tracks of CHAMP (a) and GRACE (b) satellites (top panel) and the variations of in-situ measurement of ion density (bottom panel) along the CHAMP (a) and GRACE (b) trajectories

https://doi.org/10.5194/angeo-2019-128
Preprint. Discussion started: 9 September 2019

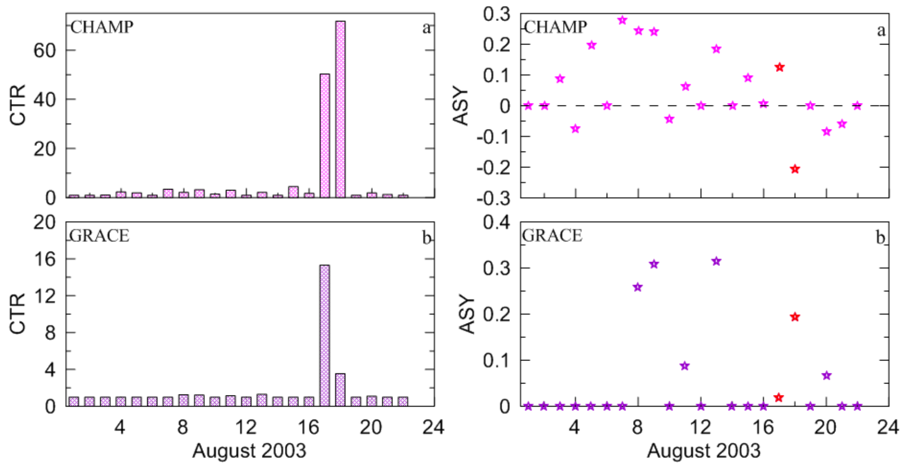

Figure 6. Variations of EIA strength (left panel) and asymmetry (right panel) during 1-22 August 2003 derived from CHAMP (a) and GRACE (b) observations in 170°E region

https://doi.org/10.5194/angeo-2019-128
Preprint. Discussion started: 9 September 2019

Annales Geophysicae
Discussions
Open Access

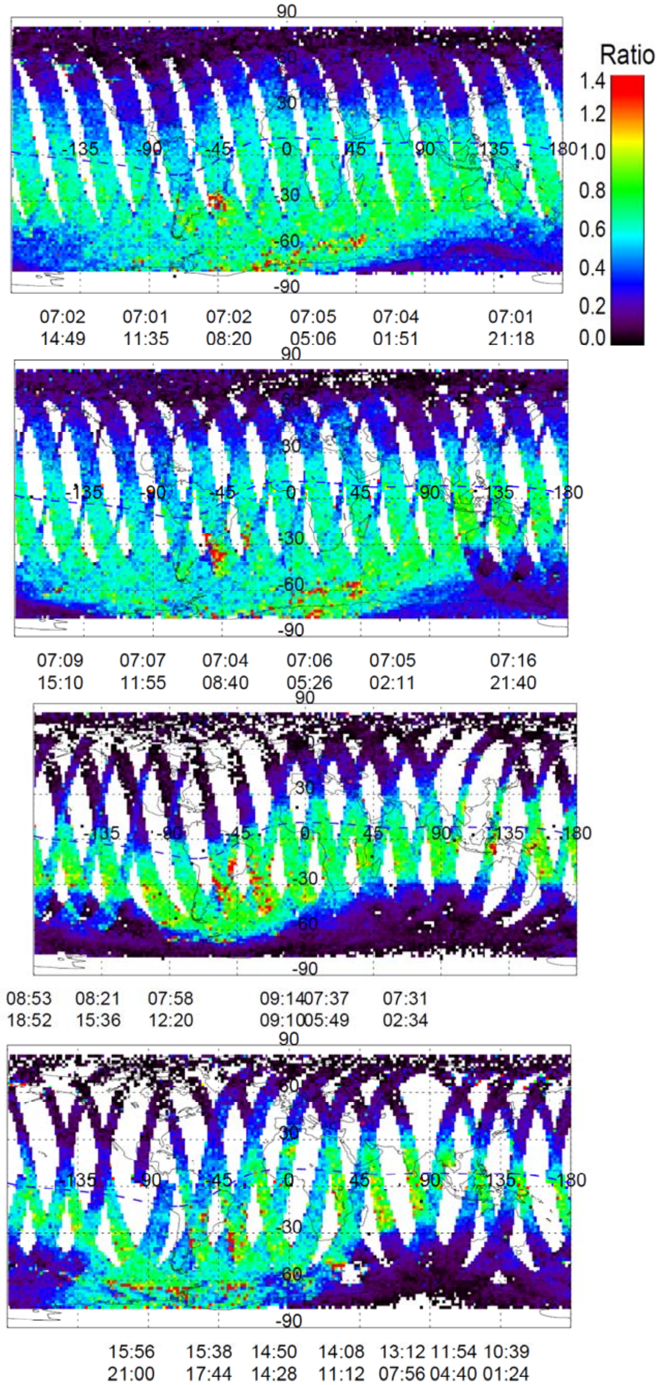

Figure 7. Variations of [O/N_2] ratio during 16-19 August 2003. From the top panel to the bottom panel, the figures represent the observations on 16 August and 19 August, respectively

https://doi.org/10.5194/angeo-2019-128
Preprint. Discussion started: 9 September 2019

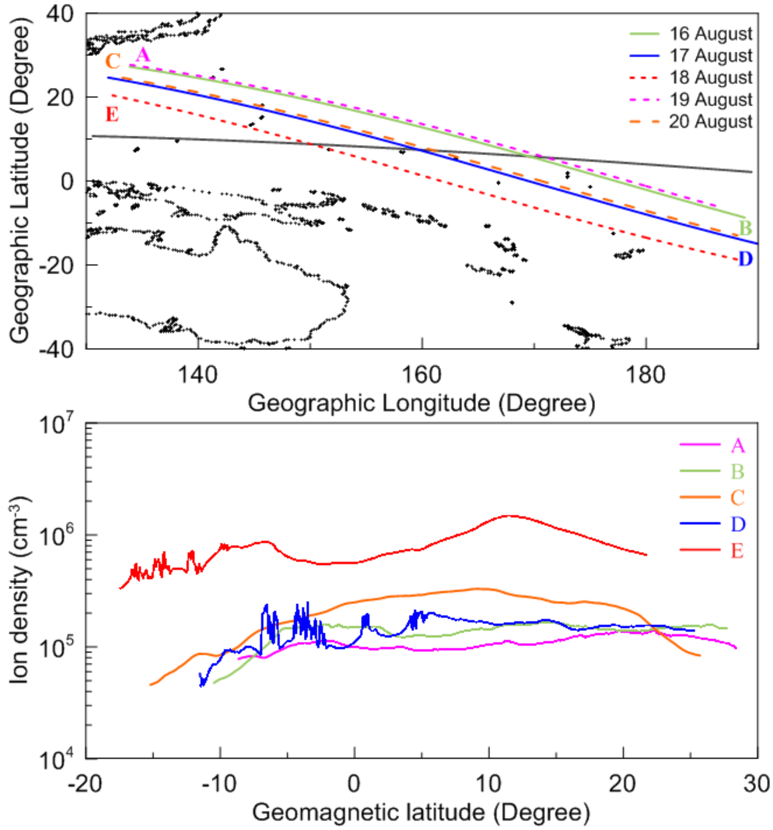

Figure 8. During 16-20 August 2003, the tracks (top panel) and density variations (bottom panel) along the ROCSAT-1 trajectories in close tracks

https://doi.org/10.5194/angeo-2019-128
Preprint. Discussion started: 9 September 2019

Annales Geophysicae
Discussions
Open Access
EGU

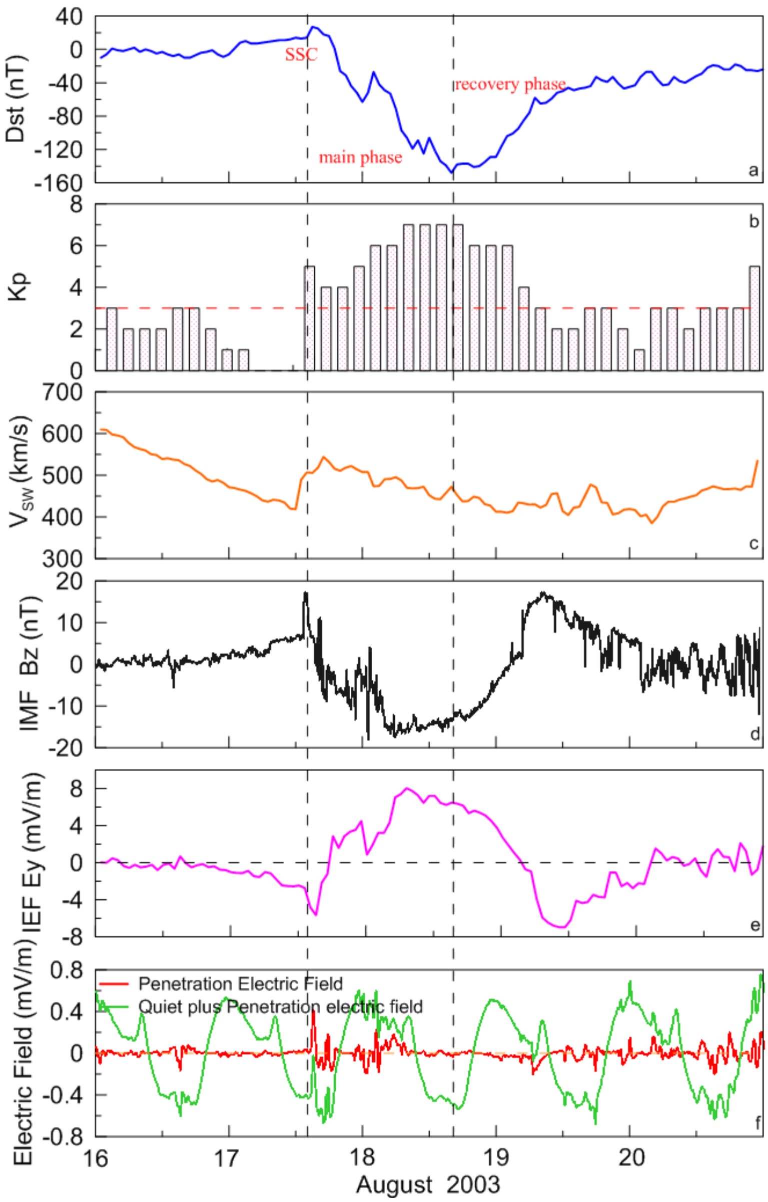

Figure 9. During 16-20 August, 2003, variations of the *Dst* index (a), K_p index (b), solar wind speed V_{SW} (c), Interplanetary Magnetic Field (IMF) B_z component (d), Interplanetary Electric Field E_y (e), and the variations of Penetration Electric Field and quiet plus penetration electric field derived from the real-time model of the ionospheric electric fields (f)